rapid decrease in intensity until about a distance of 20 cm^{-1} is reached, and also agree qualitatively with Ranganadham,[22] who obtained a maximum at the Rayleigh line of benzene and a gradual falling off of intensity from a maximum at or very near the Rayleigh line itself.

Fabelinskii[23] has obtained the orientation relaxation time in several liquids. His photographic results on CS_2 yield a relaxation time of 2.4×10^{-12} sec. Our result for the relaxation time at room temperature is 1.96×10^{-12} sec from measurement of the half-widths of the scattered light and 1.5×10^{-12} sec when measured by plotting the inverse of the intensity at different frequency shifts versus the frequency shift squared. Recent results[4] obtained with an Ar^+ laser for orientation scattering in CS_2 at room temperature differ from these results because the weak exciting source used in their experiment prevented as accurate measurements. Starunov and Zaitsev[24] have examined orientation scattering by observing the wings of the Raman and Rayleigh lines in liquids and conclude that at large frequency shifts faster processes take place such as oscillation of the molecule as a whole.

[22] S. P. Ranganadham, Indian J. Phys. **7**, 353 (1932).
[23] I. L. Fabelinskii, T. Fiz. Akad. Nauk SSSR **9**, 183 (1958).

ACKNOWLEDGMENTS

We wish to acknowledge the assistance of D. A. Jennings and M. McClintock for information on the construction of the laser and for helpful comments on the manuscript.

[24] G. I. Zaitzev and V. S. Starunov, Opt. i Spektroskopiya **19**, 893 (1964) [English transl.: Opt. Spectry. (USSR) **19**, 497 (1965)]; see also G. I. Zaitsev and V. S. Starunov, JETP Pis'ma v Redaktsiya **4**, 54 (1966) [English transl.: JETP Letters **4**, 37 (1966)].

PHYSICAL REVIEW VOLUME 154, NUMBER 1 5 FEBRUARY 1967

Mobility of Electrons in Low-Temperature Helium Gas*

JAMES L. LEVINE† AND T. M. SANDERS, JR.‡
School of Physics, University of Minnesota, Minneapolis, Minnesota
(Received 17 June 1966)

Experimental measurement of the mobility of photoelectrons in low-temperature helium gas is described. At the highest gas densities (near the normal boiling point) the mobility is lower than the value predicted by kinetic theory by four orders of magnitude. At intermediate density a transition region occurs, and at the lowest densities studied, the mobility approaches the kinetic-theory limit. A theoretical discussion of the interaction of a slow electron with a collection of helium atoms is given, and it is shown that at high density and low temperature a correlated ("bubble") state becomes thermodynamically stable. The theory predicts correctly the mobility at high density, the critical density at which the transition occurs, and the approach to the kinetic-theory value at low density. It does not, however, account for the details of the transition region. The observations, and their interpretation, provide strong support for the "bubble" model for electrons in liquid helium.

I. INTRODUCTION

THE present work, a study of electron mobilities in dense, low-temperature helium gas, was motivated by the idea that it might shed some light on the interpretation of electron and ion mobilities in liquid helium.[1]

The observation that in liquid helium the negative carrier (whether produced by ionizing radiation or by injection of photoelectrons) has a mobility somewhat below that of the positive carrier suggested that the negative carrier was not a free electron. Various possible structures appeared in the literature but were not subjected, it seemed, to very critical experimental tests. At the time when the present experiments were begun we were inclined to believe that an electron injected into helium gas would form a dense complex, bound together by electrostatic polarization. Such a structure had been suggested by Atkins[2] in connection with charged particles in liquid helium. Such a complex might also be expected to be stable in sufficiently cold and dense helium gas. At any rate, in the gaseous phase, the helium density could be varied over a wide range and the possibility of complex formation could be studied in a manner not possible in the liquid.

First measurements[3] showed that at high gas density

* This work was supported in part by the Research Corporation, the Graduate School of the University of Minnesota, and the U. S. Atomic Energy Commission.
† Present address: I.B.M. Watson Laboratory, New York, New York.
‡ Present address: Harrison M. Randall Laboratory, University of Michigan, Ann Arbor, Michigan.
[1] A survey of information on this subject, as of 1960, is given by G. Careri, in *Progress in Low-Temperature Physics*, edited by C. G. Gorter (North-Holland Publishing Company, Amsterdam, 1961), Vol. 3, p. 58.

[2] K. R. Atkins, Phys. Rev. **116**, 1339 (1959).
[3] J. L. Levine and T. M. Sanders, Jr., Phys. Rev. Letters **8**, 159 (1962).

the mobility was very low, far below the value predicted by kinetic theory. The data suggested that at high gas density the stable carrier was a heavy complex. As the gas density was lowered the mobility was observed at first to rise slowly, then precipitously, and finally to approach the kinetic-theory value at the lowest densities.

More detailed consideration of the electrostrictive complex showed that this picture could not account consistently for the data. Various other possibilities, such as negative impurity ions, were considered and rejected. Finally it appeared that a consistent and quantitative account of the data could be given in terms of the "bubble" model,[4] discussed by several authors in connection with electrons[5] and positronium[6] in liquid helium.

In the present paper we will first present our experimental results, then discuss the theory. We will show that the "bubble" model is quite consistent with our observations. We conclude that it is capable of describing the states of electrons in both liquid helium and gaseous helium at high density and low temperature.

II. EXPERIMENTAL TECHNIQUES

A. General

The mobility was measured by a time-of-flight technique similar to that of Hornbeck.[7] The arrangement is shown in Fig. 1. A short (~ 3 μsec) pulse of light is incident on the semitransparent photo surface, releasing a thin "sheet" of electrons. These drift to the anode in the applied electric field $\mathcal{E}$ and are collected, after a time ordinarily long in comparison with the duration of the light pulse. If the applied field is uniform, and effects due to space charge, diffusion, and capacitance can be neglected, the electrons will drift at a uniform velocity, giving rise to a constant current through the resistor R. The current pulse will end when the electrons reach the anode. The (small) voltage developed across R is amplified by a wide-band amplifier and displayed on an oscilloscope, and the trace is photographed. The transit time, and hence the drift velocity, are obtained from the duration of the recorded pulse. The ratio of drift velocity to field strength in the limit of zero field yields the mobility. In practice, inhomogeneities in the field distort the shape of the pulse, although an abrupt drop in current still occurs when the electrons reach the anode. This will be discussed in more detail in Sec. II E.

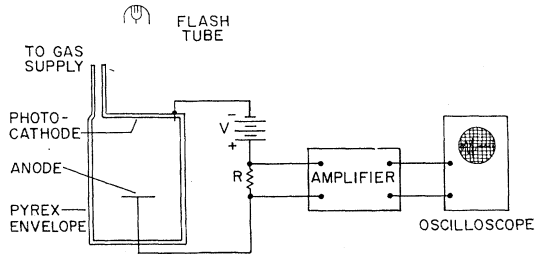

FIG. 1. Basic experimental arrangement.

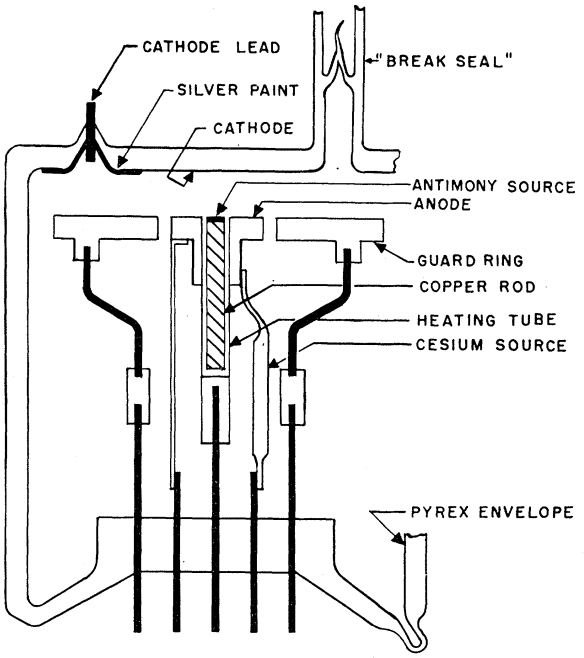

FIG. 2. Photocell construction (not to scale). The photo surface is formed by successive evaporations of antimony and cesium followed by baking at 150°C.

B. Photocell

A diagram of the photocell is given in Fig. 2. Prior to assembly, the metal parts, mostly stainless steel, were outgassed under high vacuum, the silver paste cathode connection was fired, and a semitransparent layer of platinum was evaporated onto the window and upper portion of the tube. After assembly, the cell was evacuated and baked until a vacuum of a few times 10^{-7} Torr could be maintained with the tube sealed off from the pumps. A semitransparent cesium-antimony photosurface was then formed on the window by the method described by Zworykin.[8] The underlayer of platinum was necessary for electrical contact to the photosurface at low temperatures; identical units made without backing showed a large apparent decrease in emission when cooled to 4°K. The platinum coating on the side walls of the cell prevented surface charging during a run. The resulting photosurfaces compared satisfactorily with those produced commercially. After the surface was formed, the tube was sealed off and

[4] T. M. Sanders, Jr., Bull. Am. Phys. Soc. **7**, 606 (1962).
[5] C. G. Kuper, Phys. Rev. **122**, 1007 (1959).
[6] R. A. Ferrell, Phys. Rev. **108**, 167 (1957).
[7] J. Hornbeck, Phys. Rev. **83**, 374 (1951).
[8] V. K. Zworykin and E. G. Ramberg, *Photoelectricity and Its Applications* (John Wiley & Sons, Inc., New York, 1949), pp. 96–98.

connected to the remainder of the experimental system through the break-seal shown in Fig. 2. A sputter-ion pump prevented oxidation of the photo surface when the tube was not in use.

C. Gas Handling and Cryogenics

The photocell was immersed in a bath of liquid helium during the measurements. A glass double-Dewar system of standard design was used. The bath temperature was controlled by pumping through a manostat which held the vapor pressure constant to ± 1 Torr over the temperature range 2.6–4.2°K, corresponding to a long-term temperature stability of ± 0.006°K. The vapor pressure was measured with a mercury manometer and the temperature was calculated from the 1958 E helium vapor pressure scale. The photocell was filled with high-purity helium gas evaporated from a separate reservoir of liquid. The gas handling system was pumped to a few times 10^{-6} Torr and then flushed with the purified helium before gas was admitted to the cell. The pressure in the cell was monitored with a second mercury manometer (with an accuracy of ± 1 Torr). A liquid-nitrogen cold trap prevented contamination of the cell with mercury. The fact that the cell could be reused several times without deterioration of the photosurface due to oxidation is evidence of the purity of the helium gas. Attempts to purify tank helium gas by passing it through a liquid-nitrogen-cooled charcoal trap were notably unsuccessful in this regard.

D. Electronics

The cathode voltage was supplied by a regulated power supply (500–1500 V) followed by a divider for low voltages. The cathode voltage lead was enclosed in a Pyrex tube which dipped below the level of the liquid helium, in order to prevent breakdown in the gas. The signal was fed to a Keithley model 102B wideband amplifier, using a triaxial cable. Standard feedback techniques reduced the effective input capacitance to approximately 5 pF. A 1-MΩ resistor connected across the input served as the signal resistor (R, in Fig. 1). The output was displayed on an oscilloscope with sweep speeds calibrated to 1%, and was photographed with an oscilloscope camera.

The light flash was produced by an E.G.&G. model FX-6A xenon flash tube. The discharge current was supplied by a 1-μF capacitor charged to 1 kV. The light was collected by a mirror and Lucite light pipe and was directed down a quartz light pipe to the photocell. A commercial phototube mounted near the flash tube was used to trigger the oscilloscope sweep.

E. Pulse Shape

As indicated in Sec. II A, a rectangular pulse is expected for a uniform field. The observed pulses were more complicated, as shown in Fig. 3(b). The current rises somewhat, then drops abruptly, and finally tails off rather slowly to zero. This complication is associated with the actual field distribution in the drift space, which is far from uniform. The major distortion is caused by the conductive coating on the walls of the cell, which causes the field lines to diverge outward from the anode. The field was mapped with an electrolytic tank, and the shape of the current pulse was calculated.[9] The result is shown in Fig. 3(a). The initial gradual increase is caused by an increase in drift velocity of the electrons as they approach the anode. The grounded guard ring shown in Fig. 2 collects the electrons which have gone through the worst part of the field. The peak occurs when the electrons moving down the center of the cell are first collected, and its location is not sensitive to the details of the field. The shape of the tail of the pulse was found to be very sensitive to the exact manner in which the current divides between the guard ring and the anode, and hence is not given accurately by the calculations. Let τ be the time at which the peak occurs, D the length of the drift space, and V the applied voltage. Define an average drift velocity and an average field strength by

$$\langle v_d \rangle = D/\tau, \quad \langle \mathcal{E} \rangle = V/D.$$

Then for our geometry, we find the true mobility to be given by the expression

$$\mu = 1.1 \langle v_d \rangle / \langle \mathcal{E} \rangle .$$

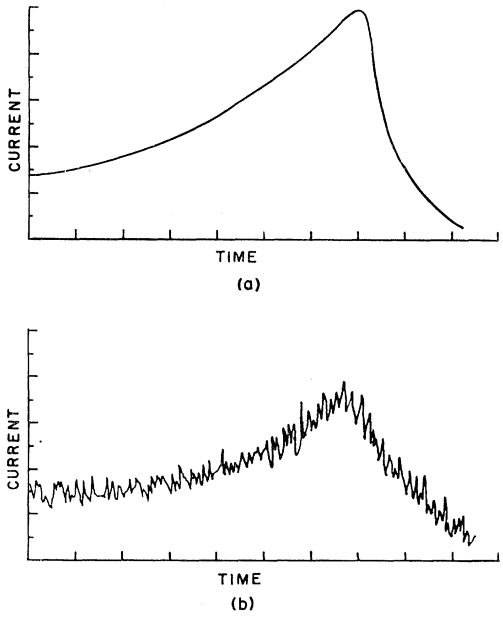

FIG. 3. (a) Calculated current pulse. (b) Typical experimental current pulse. The noise is approximately to scale but was not copied directly. Transit times are varied from a few microseconds to a few milliseconds. Peak currents were of the order of 1 nA.

[9] J. L. Levine, M.S. thesis, University of Minnesota, 1961 (unpublished).

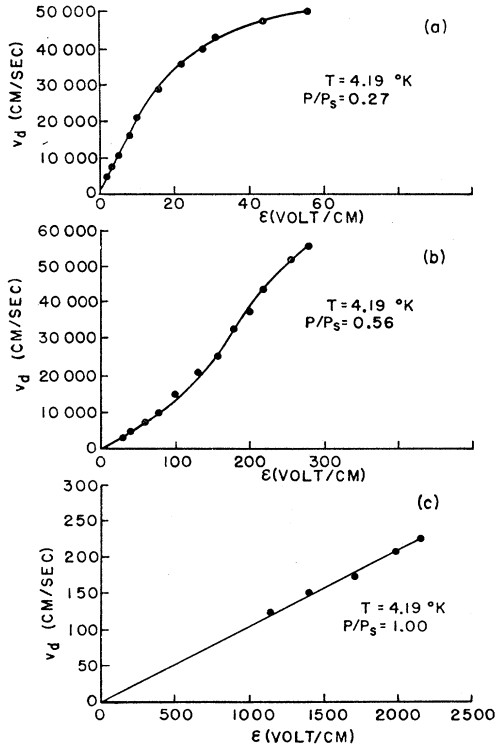

FIG. 4. Drift velocity versus field strength for the temperatures and pressures indicated. The pressures are given in units of the saturated vapor pressure p_s. Curve (a) is typical of the low-density region, curve (b) of the intermediate-density region, and curve (c) of the high-density region.

The numerical factor would be unity for a uniform field. In practice, the correction factor was not used, as the uncertainties in determining its exact value were believed to be comparable in magnitude with the correction itself.

F. Errors and Limitations

We estimate an uncertainty of $\pm 20\%$ in the absolute values of mobility and $\pm 10\%$ in relative values. These limits were set by misalignment of the electrodes, uncertainties in the electric field distribution, and uncertainties in the measurement of transit times due to noise and the finite resolving time of the equipment. In addition, the finite resolving time limited the maximum measurable mobility to about 10 000 $cm^2\ V^{-1}\ sec^{-1}$. A puzzling feature of the measurements was that the total charge actually injected into the gas increased approximately linearly with the applied voltage, and did not appear to depend on the value of the mobility. This may have been caused by space-charge effects during the light flash. On the other hand, reducing the light intensity produced a proportional decrease in the injected charge, but did not have any noticeable effect on the pulse length. As a test of the equipment, the mobility was measured at room temperature and compared with published data.[10] Our value was 12% high, within our estimated error.

III. EXPERIMENTAL RESULTS

A. General

Figure 4 shows the experimental relationship between drift velocity and field strength at $T = 4.19°K$ for several pressures. The pressures are given, in each case, in units of the saturated vapor pressure. Note that at low fields, the curves are linear and extrapolate accurately to the origin. Such a linear region was found at all pressures and temperatures; the mobility was taken from the slope of this portion of each curve. At higher fields, the curves become distinctly nonlinear [see Fig. 4(b) in particular].

B. Mobility

Figure 5 shows the mobility as a function of pressure for three temperatures. The pressures are again given in units of the corresponding saturated vapor pressure. The 4.2°K isotherm contains data taken on several runs, and with two photocells, and shows the reproducibility of the data. In Fig. 6, we show the mobility as a function of temperature at the saturated vapor pressure. Note the large variation of mobility over a narrow range

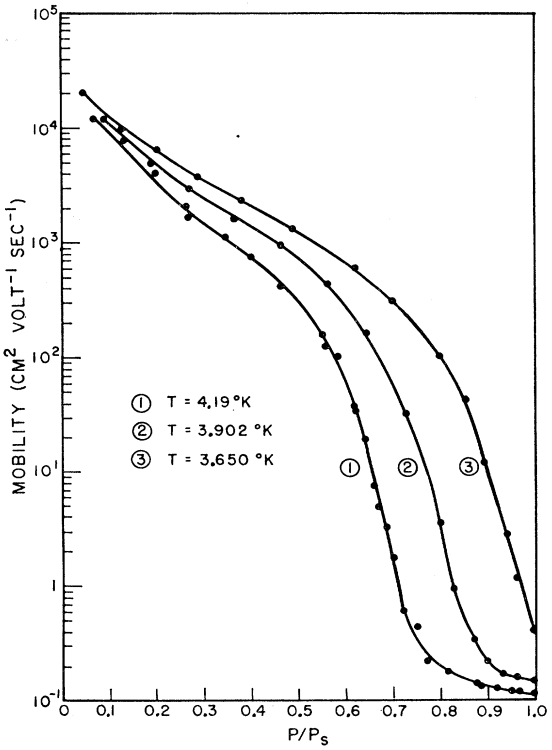

FIG. 5. Mobility versus pressure at constant temperature. The solid curves have no theoretical significance.

[10] A. V. Phelps, J. L. Pack, and L. S. Frost, Phys. Rev. **117**, 470 (1960); J. L. Pack and A. V. Phelps, *ibid.* **121**, 798 (1961).

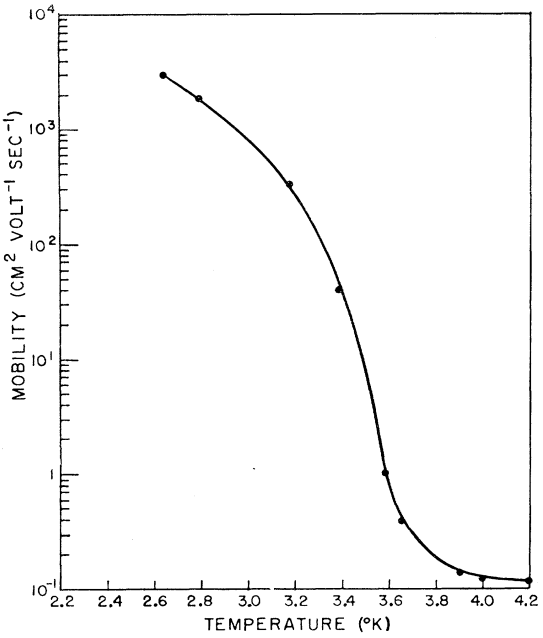

FIG. 6. Mobility versus temperature at the saturated vapor pressure. The solid curve has no theoretical significance.

of pressure or temperature in each case. At sufficiently low density, the mobility should be given correctly by the usual kinetic-theory expression [Eq. (1) below]. This expression predicts that the quantity $(T/T_0)^{1/2}\mu$ should be a universal function of the helium atom density n. In Fig. 7, we have plotted some of the mobility data in this fashion, along with a theoretical curve using the cross section given in Sec. IV.

It is evident that at low density, the mobility does approach the expected values. Further, it is clear that the mobility is essentially determined by the gas density, rather than by the pressure or temperature separately, over the entire range of our data.

IV. THEORY

A. Introduction

In this section we will discuss the theory of the interaction of an electron with a number of helium atoms. Beginning with the interaction of a low-energy electron with a single helium atom, we will show that at low gas density the states of the electrons and atoms are approximately uncorrelated, and that well-known expressions derived from kinetic theory can be used to calculate the electron mobility. This domain encompasses the region studied when electrons are injected into helium gas under normal conditions (pressure not too high, temperature not too low). On the other hand, we will show that at high gas density correlated states appear, having energies below those of the uncorrelated states. At sufficiently low temperatures and high densities these correlated states become thermodynamically stable, and the electron mobility undergoes a large change. These correlated states are of the same type as the "bubble" states discussed in connection with electrons and positrons in *liquid* helium.

B. Electron–Helium-Atom Interaction

Theoretical and experimental information concerning the interaction of a low-energy electron and a helium atom has recently been reviewed.[11,12] The interaction consists essentially of a strong short-range repulsion, arising from the Pauli principle, and a long-range polarization attraction. For electrons in the energy range of importance in this work ($E\sim10^{-3}$ eV) only s-wave elastic scattering is of any importance, and the interaction can be adequately characterized by a single parameter, the zero-energy s-wave scattering length a. We adopt for this parameter the value recommended by O'Malley,[11] $a=1.18a_0=0.62$ Å, so that $\sigma=4\pi a^2=4.9\times10^{-16}$ cm². The applicability of effective-range scattering theory to problems where the interaction includes a $1/r^4$ "tail" has already been studied.[13] It is worth noting that the s-wave scattering length is posi-

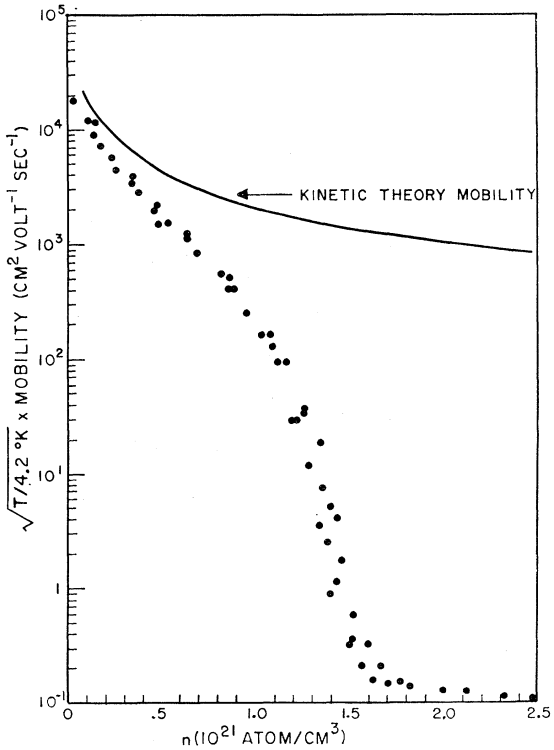

FIG. 7. A "universal" plot of mobility versus gas density. The mobilities have been multiplied by $(T/4.2)^{1/2}$ as discussed in the text. The upper solid curve was calculated from Eq. (1) of the text.

[11] T. F. O'Malley, Phys. Rev. **130**, 1020 (1963).
[12] D. E. Golden and H. W. Bandel, Phys. Rev. **138**, A14 (1965).
[13] T. F. O'Malley, L. Spruch, and L. Rosenberg, J. Math. Phys. **2**, 491 (1961); R. W. LaBahn and J. Callaway, Phys. Rev. **135**, A1539 (1964).

tive (i.e., the effective interaction is repulsive). This fact will be assumed implicitly in the following discussion. Many of the arguments may therefore not be applicable to the heavy rare gases, which have a negative scattering length and show a Ramsauer effect in low-energy electron scattering.

C. Electrons in Low-Density Helium

The mobility of electrons in low-density (e.g., NTP) helium is customarily analyzed using the Boltzmann equation, in which the electron is thought of as propagating as a free particle between collisions. When only s-wave elastic scattering is important the distinction between total cross section and momentum-transfer cross section disappears and the resultant expression for the low-field mobility is[14]

$$\mu=\frac{4}{3}\frac{e}{n\sigma(2\pi mkT)^{1/2}}. \tag{1}$$

Here μ is the mobility, n the density of scatterers (atoms), σ the total cross section, and m the electron mass.

In addition to being scattered when they are injected into a gas, the electrons experience another effect, first discussed by Fermi.[15] This second effect can be described as a shift in the zero of energy, relative to a vacuum. Alternatively, the effect can be described optically as a modification of the dispersion law for electrons in the presence of a collection of scatterers. From the optical point of view this second effect is a change in the real part of the propagation constant for electrons, caused by coherent forward scattering from the atoms. The incoherent scattering, which determines the mobility, appears as an imaginary part of the propagation constant, and corresponds to attenuation of Schrödinger waves in the medium. Derivations of the equations governing these effects appear in the literature in several places,[15–18] and will not be repeated here. We shall, however, require the results in what follows and present them below in a form convenient for our purposes.

If an electron is normally incident on a medium consisting of n randomly distributed scatterers, of scattering length a, per unit volume, and if the wave function in vacuum is

$$\psi_0=e^{ik_0z},$$

the wave function in the medium will have a gross structure of the form

$$\psi=Te^{ikz},$$

where the (complex) value of k in the medium is related to k_0 by the equation

$$k^2=k_0^2-4\pi na+i4\pi na^2k. \tag{2}$$

If we write

$$k=k_r+ik_i,$$

we obtain

$$k_i=\tfrac{1}{2}n4\pi a^2=\tfrac{1}{2}n\sigma,$$
$$k_r^2=k_0^2-4\pi na(1+\pi na^3). \tag{3}$$

We may note that inside the medium the probability density will be attenuated according to the equation

$$|\psi|^2\propto e^{-2k_iz}=e^{-n4\pi a^2z}=e^{-n\sigma z}=e^{-z/\lambda},$$

corresponding to each of the scatterers acting independently. This result does not depend on an assumption that the number of scatterers within a wavelength is small (which it is not in the present experiments) but does depend on the assumption of random spatial distribution of the scatterers. Corrections due to spatial correlations among the scatterers are discussed below. This equation justifies the use of the kinetic-theory point of view in a domain where its validity might be questioned. The equation for the real part of the propagation constant may be further simplified here, for the dimensionless parameter na^3 is very small. At the highest gas densities studied, we have

$$n\sim2\times10^{21}\ \text{cm}^{-3};\quad na^3\sim10^{-3}.$$

To a good approximation we have

$$k_r^2=k_0^2-4\pi na. \tag{4}$$

Multiplying this equation by $\hbar^2/2m$ and transposing we may rewrite this relation in the suggestive form

$$\frac{\hbar^2k_0^2}{2m}=E=\frac{\hbar^2k_r^2}{2m}+\frac{\hbar^2}{2m}(4\pi na). \tag{5}$$

Thus we may alternatively describe the effect of the medium as a shift in the zero of energy. When an electron enters a region containing scatterers of density n, the region appears like a potential barrier of height

$$V=(\hbar^2/2m)4\pi na. \tag{6}$$

In fact, from this point of view we may regard the attenuation of the wave in the medium as the result of density fluctuations, and the associated potential fluctuations. It is easy to show that in the case of a random distribution of scatterers the expression (2) results.[18]

The equation

$$V=(\hbar^2/2m)4\pi na$$

can also be readily derived by introducing an electron-atom pseudopotential and calculating the shift in energy of the electron by first-order perturbation theory. Such a perturbation calculation also justifies the use of this equation in case the density n of scatterers is not

[14] H. Margenau, Phys. Rev. **69**, 508 (1946).
[15] E. Fermi, Nuovo Cimento **11**, 157 (1934); H. Margenau and W. W. Watson, Rev. Mod. Phys. **8**, 22 (1936).
[16] L. L. Foldy, Phys. Rev. **67**, 107 (1945).
[17] E. Fermi, *Nuclear Physics* (University of Chicago Press, Chicago, 1950), p. 201.
[18] J. L. Levine, Ph.D. thesis, University of Minnesota, 1965 (unpublished).

constant in space. Some calculations of the effective-barrier height represented by a dense collection of helium atoms have recently appeared in the literature.[19,20] At a density corresponding to that of liquid helium (an order of magnitude larger than encountered in the present work), the first-order expression (6) is too low by a factor of approximately 2. This conclusion is in agreement with experimental data also.[21,22] These high-density calculations provide additional support for the use of Eq. (6) in the density range of concern here. Finally, we may note that spatial correlations among the scatterers can be taken into account in evaluating the incoherent scattering in a manner identical to that used in the analysis of scattering of electromagnetic waves. The result is also identical, namely,[23]

$$k_i=\tfrac{1}{2}n\sigma\left[kT\Big/\left(\frac{\partial p}{\partial n}\right)_T\right], \tag{7}$$

where the factor in brackets is equal to unity for a material obeying the ideal gas law. In the domain of the present work ($2.2°\mathrm{K}<T<4.2°\mathrm{K}$; $p<1$ atm) this correction is sometimes appreciable and can be evaluated from known equation-of-state data.[24]

D. Electrons in Dense Helium

1. The Ground State—A Model Calculation

The effects discussed in the previous section, in particular the shift in the zero of energy of an electron when it is in a region containing scatterers, can lead to qualitative changes in the behavior of the system when the density of scatterers becomes high. Before proceeding to the real problem, namely a number of electrons in a real (nonideal) gas at finite temperature, we will discuss briefly a model calculation. The model exhibits some features which will be of interest later, and is more amenable to simple discussion.[24a]

We consider a single electron of mass m, and N atoms (bosons) of mass M, in a volume V. We suppose the atoms not to interact with each other, but to interact with the electron via a short-range repulsion which we represent by the pseudopotential

$$V(\mathbf{r}-\mathbf{R}_i)=(\hbar^2/2m)4\pi a\delta(\mathbf{r}-\mathbf{R}_i). \tag{8}$$

We look for the lowest energy solution of the Hartree (or Hartree-Fock) equations for the system wave function, assumed to be of the form

$$\Psi(\mathbf{r},\mathbf{R}_1,\mathbf{R}_2,\cdots,\mathbf{R}_N)=\varphi(\mathbf{r})\prod_{i=1}^{N}\psi(\mathbf{R}_i). \tag{9}$$

φ and ψ satisfy the equations

$$\begin{aligned}&-\frac{\hbar^2}{2m}\nabla_r^2\varphi+\frac{\hbar^2}{2m}4\pi aN|\psi(\mathbf{r})|^2\varphi-\epsilon\varphi=0,\\&-\frac{\hbar^2}{2M}\nabla_R^2\psi(\mathbf{R})+\frac{\hbar^2}{2m}4\pi a|\varphi(\mathbf{R})|^2\psi(\mathbf{R})-W\psi(\mathbf{R})=0.\end{aligned} \tag{10}$$

These equations are clearly satisfied by

$$\begin{aligned}\varphi&=(1/V^{1/2})e^{i\mathbf{k}\cdot\mathbf{r}},\\\psi&=(1/V^{1/2})e^{i\mathbf{K}\cdot\mathbf{R}},\end{aligned} \tag{11}$$

for which $|\varphi|^2$ and $|\psi|^2$ are independent of position. For the lowest state of the system ($k=K=0$) we have

$$E_u=\langle\mathcal{H}\rangle=\frac{\hbar^2}{2m}(4\pi a)\frac{N}{V}=\frac{\hbar^2}{2m}(4\pi na), \tag{12}$$

in agreement with the results quoted in the previous section. We shall refer to this state as "uncorrelated." We can approximately satisfy the Hartree equations with a different type of trial function as well. Suppose we take again

$$\Psi(\mathbf{r},\mathbf{R}_1,\cdots,\mathbf{R}_N)=\varphi(\mathbf{r})\prod_i\psi(\mathbf{R}_i),$$

with φ and ψ now free-particle functions in part of the volume and zero elsewhere. Thus we may try

$$\begin{aligned}\varphi(\mathbf{r})&=A\frac{\sin k(r-b)}{r}, && r<b\\&=0, && r>b,\end{aligned} \tag{13}$$

$$\begin{aligned}\psi(\mathbf{R})&=B\frac{\sin K(R-b)}{R}, && R>b\\&=0, && R<b.\end{aligned} \tag{14}$$

For these functions the interaction terms in the Hartree equations vanish everywhere, and the energy of the system is

$$E_c=\langle\mathcal{H}\rangle=\frac{\hbar^2}{2m}k^2+N\frac{\hbar^2}{2M}K^2 \tag{15}$$

with $k=\pi/b$.

The lowest value of K is readily determined, and for periodic-type boundary conditions on a sphere of radius L (i.e., $d\psi/dR=0$ at $R=L$) takes the form

$$K^2=3b/L^3.$$

[19] B. Burdick, Phys. Rev. Letters **14**, 11 (1965).
[20] J. Jortner, N. R. Kestner, S. A. Rice, and M. H. Cohen, J. Chem. Phys. **43**, 2614 (1965).
[21] W. T. Sommer, Phys. Rev. Letters **12**, 271 (1964).
[22] M. A. Woolf and G. W. Rayfield, Phys. Rev. Letters **15**, 235 (1965).
[23] J. O. Hirschfelder, C. F. Curtiss, and R. B. Bird, *Molecular Theory of Liquids and Gases* (John Wiley & Sons, Inc., New York, 1954), p. 896.
[24] W. E. Keller, Phys. Rev. **97**, 1 (1955); J. F. Kilpatrick, W. E. Keller, and E. F. Hammel, *ibid.* **97**, 9 (1955).
[24a] Related calculations are summarized by E. P. Gross, in *Proceedings of the Sussex University Symposium on Quantum Fields*, edited by D. F. Brewer (North-Holland Publishing Company, Amsterdam, 1966), p. 275; see also R. C. Clark, Phys. Letters **16**, 42 (1965).

In deriving this expression we have assumed $b \ll L$. Expression (15) for the energy then becomes

$$E_c = \frac{\hbar^2}{2m}\left(\frac{\pi}{b}\right)^2 + \frac{\hbar^2}{2M}(4\pi n b),$$

where we have written

$$n = N/\tfrac{4}{3}\pi L^3.$$

We may now regard b as a variational parameter and find both the value of b which minimizes E_c and the corresponding minimum energy. The results are

$$b_m^3 = \pi M/2mn, \tag{16}$$

$$E_{cm} = \frac{3\hbar^2\pi}{M}\left(\frac{\pi n^2 M}{m}\right)^{1/3}. \tag{17}$$

Accordingly the ratio of the energy of the correlated ground state (17) to that of the uncorrelated ground state (12) is given by

$$\left(\frac{E_{cm}}{E_u}\right)^3 = \frac{27\pi}{8}\left(\frac{m}{M}\right)^2\left(\frac{1}{na^3}\right). \tag{18}$$

Thus E_{cm} will be less than E_u for sufficiently large density. The quantitative criterion is

$$E_{cm} < E_u$$

for

$$na^3 > \frac{27\pi}{8}\left(\frac{m}{M}\right)^2. \tag{19}$$

Inserting numerical values for electrons and helium atoms we obtain

$$E_{cm} < E_u$$

for

$$n > 10^{18}\ \text{cm}^{-3}.$$

The result, which pertains to the ground state only, does not, of course, imply that these correlated states will dominate at finite temperature whenever n is larger than 10^{18} cm^{-3}. The domain in which these correlated states will be statistically preferred will be discussed in the following section. As a concluding remark we may note that the calcualtion of the present section can also be carried through using box boundary conditions (i.e., $\psi = 0$ at $R = L$). In this case the uncorrelated state does not satisfy the Hartree equations exactly because of the somewhat unphysical variation in density across the box. For this reason, we have preferred the periodic-type boundary conditions, although the results of the two calculations are essentially the same.

2. *Stability of the Correlated State at Finite Temperature*

In the previous section we have demonstrated, in a model problem, the existence of correlated states which can have energies well below those of the customary uncorrelated states. Both that calculation and those of the present section are essentially variational in character. That is to say they establish the existence of states below the normal uncorrelated ones, but the question of whether these correlated states are well-represented by the wave functions here employed must be regarded as open, pending a solution of the real many-body problem. It may be noted, however, that the correlated wave functions have the characteristics of bound states and are very likely not readily susceptible to analysis through use of perturbation theory.[25]

We now address ourselves to the problem of an electron, or a very dilute gas of electrons, immersed in helium gas at finite temperature. Interactions among the helium atoms will be accounted for approximately, insofar as they affect the equation of state of the gas. Our model of the correlated states is basically that of the previous section. We suppose the density of helium atoms to be constant outside a sphere of radius b and zero inside. The results of Sec. IV C show that such a density distribution appears to an electron to be a spherical square well of radius b and height $V = (\hbar^2/2m) \times 4\pi na$. Whatever the value of n, there will be bound-state solutions of the Schrödinger equation when b is sufficiently large. The ratio of the number of electrons to be found in these correlated (or "trapped") states (N_t) to the number in the uncorrelated (or "free") states (N_f) is given by

$$N_t/N_f = e^{\Delta F/kT}, \tag{20}$$

where ΔF is the change in free energy of the system associated with a transition of an electron from a free state to a trapped state. We write

$$\Delta F = \Delta F_{\text{el}} + \Delta F_{\text{gas}}, \tag{21}$$

where the interaction energy between electrons and gas atoms will be included in ΔF_{el}. ΔF_{gas} is readily evaluated, since in the trapped state the gas is excluded from the volume of a sphere of radius b. Thus we have

$$\Delta F_{\text{gas}} = \left(\frac{\partial F}{\partial V}\right)_T (-\tfrac{4}{3}\pi b^3) = \tfrac{4}{3}\pi b^3 p. \tag{22}$$

We are, however, only partially successful in evaluating the free-energy change of the electron.

Writing $\Delta F_{\text{el}} = \Delta E_{\text{el}} - T\Delta S_{\text{el}}$, we have $\Delta E_{\text{el}} = -E_b$, where E_b is the binding energy of the electron in the spherical square well of height V and radius b. This quantity is readily evaluated, although no closed expression can be given. We have not succeeded in evaluating ΔS_{el}, whose determination requires a knowledge of the density of states of the system for electrons in the trapped states. We will discuss this quantity somewhat speculatively below, concluding that it is unlikely to change any of our results qualitatively. Meanwhile, we

[25] M. Coopersmith, Phys. Rev. **139**, A1359 (1965).

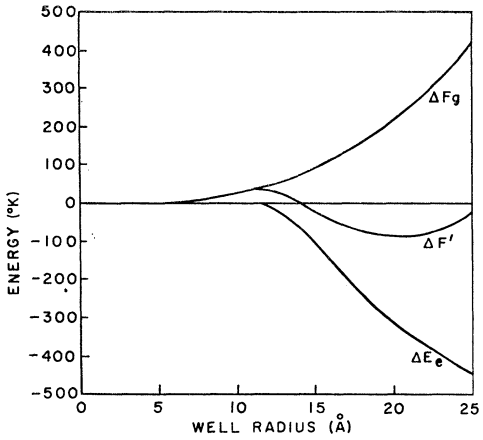

FIG. 8. The quantities ΔF_{gas}, ΔF_{el}, and $\Delta F'$ as functions of square-well radius b, for $T=4.2°\text{K}$ and the saturated vapor pressure.

may examine the behavior of the quantity

$$\Delta F'=\Delta F+T\Delta S_{\text{el}}=\Delta F_{\text{gas}}+\Delta E_{\text{el}}$$
$$=\tfrac{4}{3}\pi b^3 p-E_b. \tag{23}$$

In Fig. 8 we show, as functions of b, the quantities ΔF_{gas}, ΔE_{el}, and $\Delta F'$ for $T=4.2°\text{K}$ and $p=1$ atm. In Fig. 9, we show $\Delta F'$ versus b for $T=4.2°\text{K}$ and several pressures. When the density is large and the pressure not too large (i.e., at high n and low T) the plot of $\Delta F'$ versus b shows a well-defined minimum with $\Delta F'$ negative near the minimum. As the density is lowered, at fixed T, the value of $\Delta F'$ increases and the minimum becomes shallower until a critical value of the density is reached, below which there is no minimum.

We now return briefly to a discussion of the terms omitted so far in the calculation of ΔF, the free-energy change associated with bubble formation. We must evaluate the change in the entropy of the electron,

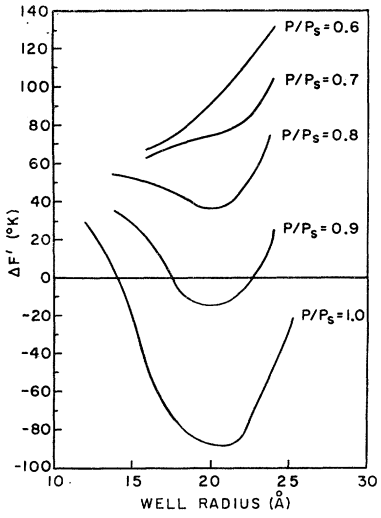

FIG. 9. The partial free energy $\Delta F'$ as a function of square-well radius b, for $T=4.2°\text{K}$ and for the pressures indicated. The pressures are given in units of the saturated vapor pressure p_s.

associated with the process. There are at least two contributions which we can estimate, but we are not able to give a complete calculation of the entropy change. The first contribution comes from the fact that the density of translational states depends upon the mass of a particle. If we apply the customary ideal gas theory to the electrons, this makes a contribution $\Delta F_t=-\frac{3}{2}kT\times\ln(m^*/m)$. Here m^* is the effective mass of the bubble, and m the free-electron mass. The result is only logarithmically dependent on the mass, and will be very slowly varying. If we use as a mass estimate one-half the mass of the displaced atoms, the numerical value of this term, at 4.2°K and 1 atm, is $\Delta F_t/k\cong-80°\text{K}$. Adding this contribution to $\Delta F'$ would have the effect of lowering all the curves of Fig. 9 by approximately this amount so that all the minima shown would occur at negative values of ΔF. There will be an additional contribution to ΔF from the vibrational degrees of freedom of the bubble. This will have the effect of making ΔF still more negative at the minimum. In Hooke's law approximation, each normal mode contributes a term $\Delta F_v=kT\ln(\hbar\omega_0/kT)$ to the free energy. We have assumed $\hbar\omega_0<kT$ in writing this expression. For the spherically symmetrical mode, for example, this amounts to $\Delta F_v/k\cong-10°\text{K}$.

Thus the effect of these contributions to ΔF is to lower all free-energy curves to such an extent that whenever the free-energy curve has a minimum the value of the free energy is lowered by bubble formation. In the discussion which follows we will assume this, but we will not otherwise be dependent on an understanding of these contributions to the free energy.

We assume further that the bubble states are not important when the free-energy curve has no minimum. Under these conditions a bubble, if formed, will collapse and eject the electron.

E. Self-Consistency of Model

In calculating the wave function and binding energy of an electron in a "bubble" state, we made use of a rather simple form for the density disturbance in the gas, a square well whose radius was to be adjusted to minimize the over-all free energy. This is certainly an oversimplification. In this section we will derive a self-consistent set of equations for the electron wave function φ and the gas density $n(\mathbf{R})$. We assume that the electron wave function will adjust itself to the average position of the gas atoms given by $n(\mathbf{R})$. Therefore, φ will be a solution of an effective Schrödinger equation,

$$-\frac{\hbar^2}{2m}\nabla^2\varphi+V\varphi=E\varphi;\quad V=\frac{2\pi\hbar^2 a}{m}n(\mathbf{R}). \tag{24}$$

At the same time, we assume that the gas density will adjust itself to minimize the free energy. Using the pseudopotential [Eq. (6)] we can calculate the interaction

energy of an atom located at position $\mathbf{R}$,

$$\langle V_{\text{int}}\rangle=\frac{2\pi\hbar^2 a}{m}|\varphi(\mathbf{R})|^2. \tag{25}$$

Then a straightforward calculation shows that $n(\mathbf{R})$ is given by

$$kT\ln\frac{n(\mathbf{R})}{n_0}+2kTB(T)[n(\mathbf{R})-n_0]=-\frac{2\pi\hbar^2 a}{m}|\varphi(\mathbf{R})|^2. \tag{26}$$

Here, $B(T)$ is the second virial coefficient. n_0 is determined by requiring that the volume integral of $n(\mathbf{R})$ yield the number of atoms. Dropping small terms, we find

$$n(\mathbf{R})=n_0\exp\left\{-\frac{2\pi\hbar^2 a}{mkT}|\varphi(\mathbf{R})|^2\right\}. \tag{27}$$

Equations (24) and (27) form a highly nonlinear set of equations which we have not attempted to solve directly. We regard the square well and its associated wave function as a trial solution for this set of equations. In Fig. 10, we show the initial square well, the square of the electron wave function, and the density function calculated by substituting the wave function into Eq. (27), plotted as functions of R. The agreement between the initial and recalculated density functions is fair. We have multiplied $|\varphi(\mathbf{R})|^2$ by $(2\pi\hbar^2 a/mk)$ in plotting Fig. 10(b) so that this figure represents the interaction energy of an atom, measured in temperature units. We see that the classical turning radius of a 4°K thermal atom approaching the electron is approximately 16 Å. Therefore, the "bubble" will behave somewhat like a (soft) sphere of this radius. We will use this radius in estimating the mobility.

F. Calculation of the Mobility of a "Bubble" Ion

In this section we will estimate the mobility of a trapped or "bubble" ion. We base our calculation on the result of the previous section, that the ion should behave approximately like a sphere of radius ≈ 16 Å. Unfortunately, at the gas densities of interest, the mean free path for atom-atom collisions (λ_g) is ~ 10 Å, so that neither kinetic theory nor classical hydrodynamics applies accurately. We will therefore make use of an interpolation formula which has been known for some time.[26] We must first discuss briefly the effective mass of the bubble. If the situation were described adequately by classical hydrodynamics, the carrier would have an effective mass of one-half the mass of the gas displaced, approximately 20 helium atom masses for the ions under consideration. Since classical hydrodynamics is only approximately applicable, this is only a rough estimate. However, in the formula to be given for the mobility, the reduced mass between an ion and a helium atom enters. As a result, the effective mass appears only weakly in the final result as long as it is large compared to the atomic mass.

[26] A. M. Tyndall, *The Mobility of Positive Ions in Gases* (Cambridge University Press, New York, 1938).

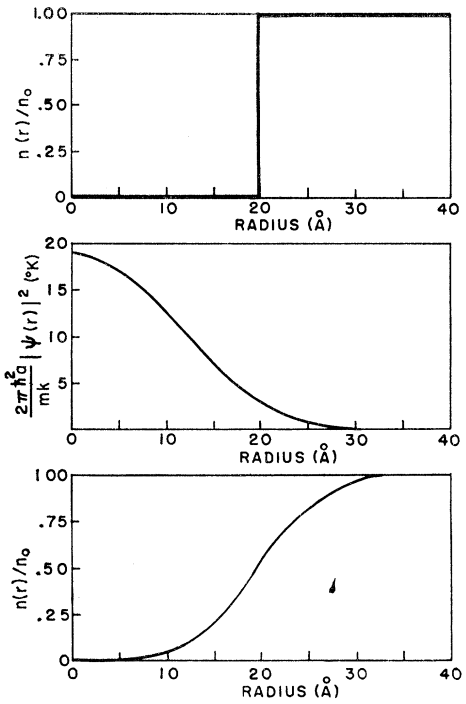

FIG. 10. (a) Square well pertinent to the discussion of Sec. IV E. (b) Electron wave function, squared. (c) Density calculated from Eq. (27), to be compared with the square well. The conditions correspond to $T=4.2$°K and the saturated vapor pressure.

The interpolation formula is arranged so that it reduces to the appropriate expression for the mobility in the regions where kinetic theory or hydrodynamics becomes applicable,

$$\mu=\frac{e}{6\pi\eta R}\left[1+\frac{9\pi\eta}{4nR(2\pi MkT)^{1/2}}\right]. \tag{28}$$

Here η is the viscosity, and we have assumed that the reduced mass of the ion is equal to the helium atomic mass. For a gas of (classical) hard spheres, this may be written as

$$\mu=\frac{e}{6\pi\eta R}\left(1+\frac{45T\sqrt{2}}{128}\frac{\lambda_g}{R}\right). \tag{29}$$

Equation (28) is applicable to real gases.

V. INTERPRETATION OF DATA

A. Low-Field Mobilities

The data presented in Sec. III show that the mobility of electrons in low-temperature helium gas is consist-

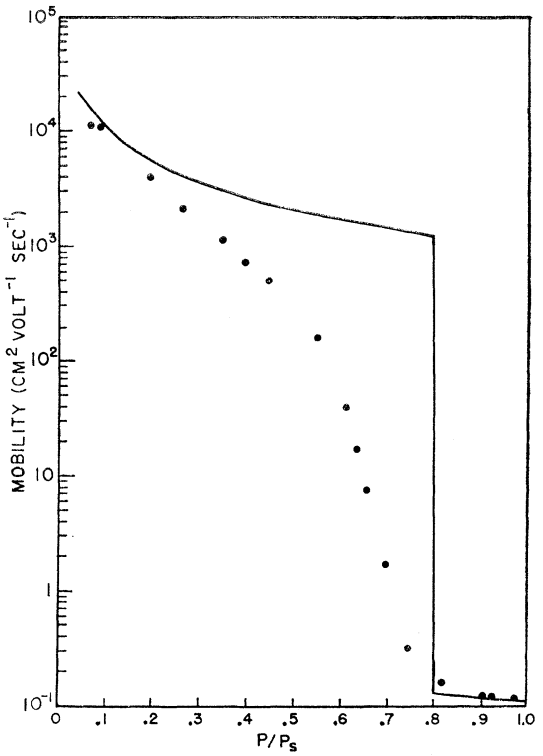

FIG. 11. Variation of mobility with pressure at 4.2°K. The circles are data points. The curve is calculated in the manner described in Sec. V A.

ently lower than predicted by normal kinetic-theory considerations [Eqs. (1) and (7)]. At the highest densities the mobility lies below the kinetic-theory value by a factor of approximately 10^4. As the density is lowered the mobility rises rapidly, approaching the kinetic-theory value at the lowest density studied (see Fig. 7).

The theory described in Sec. IV predicts that in the high-density region the stable state of the electron is one in which the electron wave function is localized in a "bubble." Equation (28) of Sec. IV F permits us to calculate the approximate mobility of a "bubble" in terms of its equilibrium radius (see Fig. 9) and known properties of helium gas.

The theory given in Sec. IV also permits us to calculate the mobility of the "free" electrons [Eq. (1)] and the relative probability of finding an electron in a "free" state or a "trapped" state. If we assume that in the intermediate range, where the electron is not overwhelmingly in one state or the other, an electron makes many transitions between the two states during the time required to traverse the drift space, then we can calculate the mobility for all densities from the equation

$$\mu = p_f \mu_f + p_t \mu_t. \tag{30}$$

Here, μ_f and μ_t are the mobilities of free and trapped electrons and p_f and $p_t = (1-p_f)$ are the probabilities of finding an electron in the free state and the trapped state. The mobility–versus–pressure curve for $T = 4.2$°K predicted by Eqs. (1), (28), and (20) is plotted in Fig. 11. It can be noted that the major qualitative features of the data are consistent with the theory. First, the mobility at high density is in rather good agreement with the approximate theory of Sec. IV F. Second, a very rapid rise to the kinetic-theory mobility is predicted at approximately the correct value of the pressure. In quantitative detail, however, the theory predicts that the transition from the trapped-electron behavior to the free-electron behavior occurs over a much narrower density range than is observed. The reason for this is that the quantity ΔF of Eq. (20) need only change by a few times $kT \sim 10^{-3}$ eV to cause the transition to be nearly complete, and the terms contributing to ΔF are so large that this small change in ΔF occurs over a very narrow density range. We can only make some rather speculative remarks about the actual state of affairs in the transition region, in which the mobility is rapidly varying. We assume that the fact that the mobility in this transition region is low implies that the motion of the electron does involve some correlated motion of helium atoms. The theory of Sec. IV implies that the electron–helium-atom interaction is not strong enough to produce thermodynamically stable bound states at the densities involved here. In this domain the free energy of the trapped state may be lower than that of the free state, but the free-energy–versus–bubble-radius curves do not have minima.

B. High-Field Effects

At the highest gas densities studied, the range of electric fields available limited us to the region where the drift velocity of the charges was proportional to the electric field strength. At the lowest densities, the behavior was that normally observed for "hot" free electrons, although in this region the transit times became so short that instrumental resolving times severely limited the region we could study. In the intermediate-density region, where the mobility is strongly density-dependent, the electric field dependence of the mobility was quite anomalous [see Fig. 4(b)]. The high-field data can be collected together and compared by making use of a different type of display. The ratio of the drift velocity to the thermal velocity should be a universal function of the dimensionless parameter $e\mathcal{E}\lambda/kT$ for free electrons in helium gas. That is, data taken at arbitrary values of $\mathcal{E}$, p, and T will lie on the same curve, provided the electrons are correctly described by the usual kinetic-theory assumptions. In Fig. 12, we display our high-field data on such a plot. The solid curve is obtained from accurate room-temperature measurements.[10] The low-field region, where the electrons are still in thermal equilibrium, is characterized by v_d proportional to $\mathcal{E}$. At high fields the electron velocity distribution is determined by $\mathcal{E}$, and v_d is proportional to $\mathcal{E}^{1/2}$. The experimental data, shown

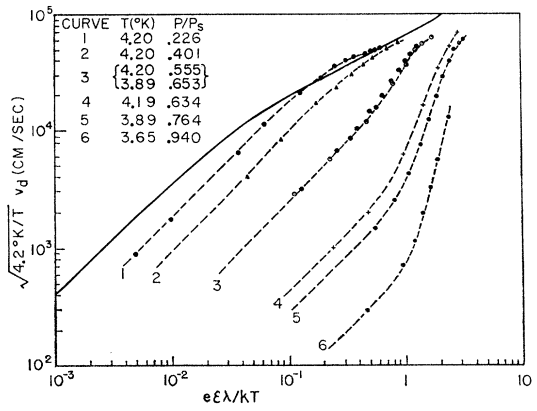

FIG. 12. "Universal" curve for "hot" electrons in the kinetic-theory regime. The heavy solid curve is obtained from room-temperature data. The circles are data points; the smooth curves passing through them are intended as guides for the eye.

by dashed curves in Fig. 12, all show low-field drift velocities below the kinetic-theory value, but appear to converge to the universal curve for "hot" free electrons at sufficiently high electric fields. Evidently the correlation between an electron and a helium atom, which lowers the mobility below the kinetic-theory values in the intermediate-density region, is dependent on electron energy. As the electron energy is raised, in the high-field region, the correlation becomes weaker and weaker until, at the highest fields, the behavior is that expected for free electrons. We have not succeeded in extracting quantitative information out of the high-field phenomena.

VI. CONCLUSIONS

The experimental results reported here show that the mobility of electrons injected into dense helium gas at low temperatures is very anomalous. At the highest densities the mobility is that of a heavy complex. After a transition region at intermediate density, the mobility approaches the expected kinetic-theory value at the lowest density studied.

This behavior, including the values of the mobility in the high- and low-density regimes, and the critical value of the density at which the transition occurs, is shown to be understandable in terms of the known interaction of slow electrons and helium atoms. At high densities a "bubble" state, similar to that previously discussed in connection with electrons and positronium in *liquid* helium, is thermodynamically stable. At lower density a rapid transition to the kinetic-theory regime is predicted. In the transition region a weakly correlated state is evidently present. The experimental data at high electric fields show that this correlation becomes weaker as the electron temperature is raised, but do not elucidate completely the nature of this intermediate state.

None of the other models considered is able to account for the observed variation of mobility with gas density.

The data, and their interpretation, provide strong support for the "bubble" model for electrons in liquid helium.

ACKNOWLEDGMENTS

We wish to acknowledge the assistance of A. J. Dahm and J. Herian in connection with the experiments described here. The glassblowing required in the fabrication of the phototubes was performed by E. Greinke and M. Dynes.

During part of the period in which this work was performed one of us (J. L. L.) was a National Science Foundation Cooperative Predoctoral Fellow, and the other (T. M. S.) was an Alfred P. Sloan Foundation Fellow.